Relaxation Oscillations in Chemical Reactors

E. D. GILLES
GERHART EIGENBERGER
and
WILHELM RUPPEL

Institut fur Systemdynamik und Regelungstechnik
Universität Stuttgart
Pfaffenwaldring 9, D-7000 Stuttgart 80, West Germany

This paper deals with a particular type of limit cycle in chemical reaction systems, the so-called relaxation oscillation. This phenomenon can be caused by thermal or kinetically induced instabilities in a loop reactor or a CSTR, but can also occur in a catalytic fixed-bed reactor for an endothermic reaction with self-inhibiting or self-accelerating steps.

SCOPE

Currently, a number of oscillating chemical reactions are known in homogeneous, heterogeneous, and biological systems, such as the bromate-cerium-malonic acid system, the oxidation of carbon monoxide on platinum, or the glycolysis. All these reactions were discovered by chance and led to a large number of publications concerning explanations of these phenomena.

The shape of these oscillations bears no resemblance to harmonic functions; rather, it is signified by periodic jumps or saw toothed oscillations, the so-called relaxation oscillations.

This paper shows, with the aid of three examples, that relaxation oscillations can also occur as a result of the interaction of mass and heat transport processes with relatively simple reactions. These examples are, firstly, a first-order exothermic reaction on a catalyst pellet in a loop reactor as published by Horak and Jiracek (1972), secondly, a hypothetical surface reaction in a stirred-tank reactor under isothermic conditions, and, finally, an endothermic reaction with self-inhibiting steps in a fixed-bed reactor.

CONCLUSIONS AND SIGNIFICANCE

Contrary to general opinion, multiple steady states and oscillations can also occur in endothermic reactions through the interaction of transport processes and reaction in a fixed-bed reactor. Prerequisite is a reaction with self-inhibiting or self-accelerating steps.

This paper, taking as an example an endothermic reaction with self-inhibition, shows, by means of simulation results, the buildup of relaxation oscillations in both a differential reactor and a fixed-bed reactor of finite length. The simulation was based on the dehydrogenation of an alcohol on an oxide catalyst. However, in this paper the actual reaction rate was simplified in order to show the basic behavior more clearly.

The treatment of a differential reactor leads to a graphical stability criterion for a fixed-bed reactor of finite length. Based upon the two phase model, the spatial profiles of the temperature and concentration inside the reactor were calculated. The result is a periodic ignition and extinction of the reactor with very steep and creeping concentration profiles within the catalyst.

Recently, the occurrence of relaxation oscillations in chemical reactors has been pointed out by Gilles and Eigenberger (1976). Such instabilities can generally occur in nonlinear systems characterized by one relevant storage. As an example, the following second-order system will be considered:

$$\frac{dx_1}{dt} = f_1(x_1, x_2) \tag{1}$$

$$\epsilon \frac{dx_2}{dt} = f_2(x_1, x_2) \tag{2}$$

where f_1 is linear in x_1, x_2 and $f_2 = 0$ exhibits multiple solutions as shown in Figure 1. If ϵ is very small, x_2 attains its steady state rapidly. Then all phase trajectories are vertical lines which approach the lower and upper branch of the steady state solution $f_2 = 0$.

The middle branch (dashed line) of Figure 1 is unstable. If the only steady state of the whole system [Equations (1) and (2)] lies on the unstable branch (Figure 2), the depicted limit cycle will develop where x_2 changes jumpwise from the upper to the lower branch and vice versa.

Correspondence concerning this paper should be addressed to E. D. Gilles. G. Eigenberger is with BASF AG., Ludwigshafen, Abt. TEI.

0001-1541-78-8511-0912-$01.05.

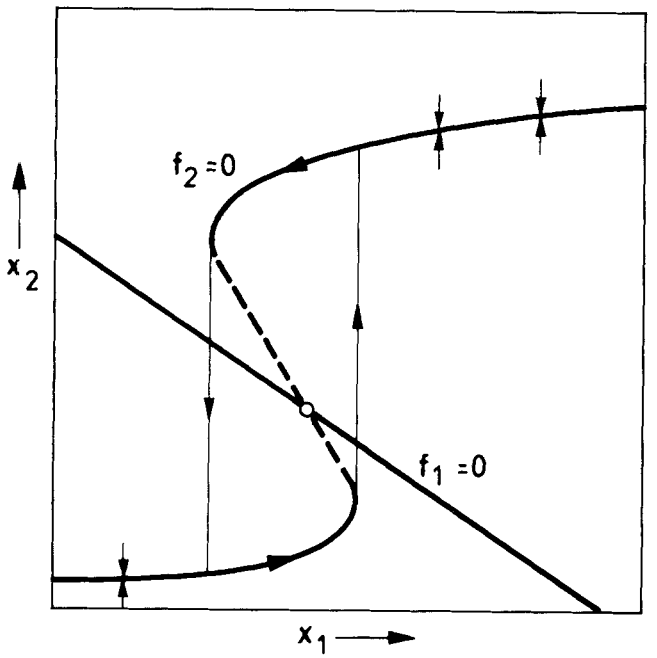

Fig. 1. Phase plane of the system, Equations (1) and (2).

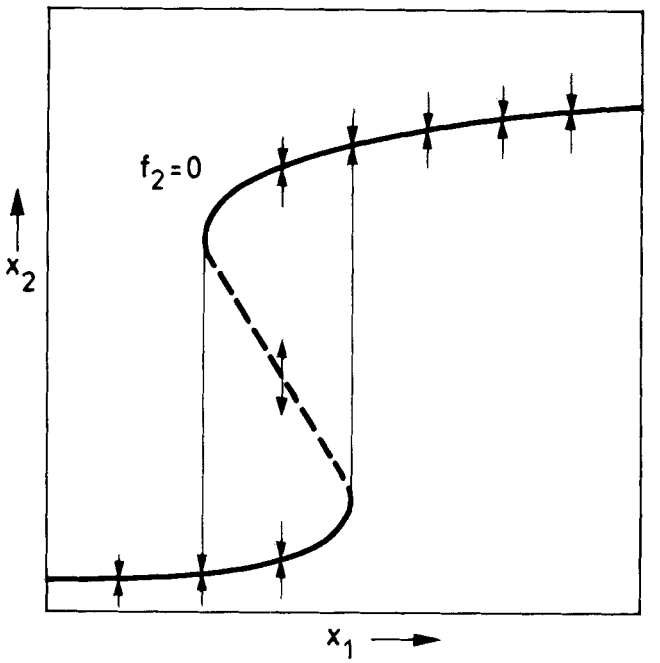

Fig. 2. Steady state solution and limit cycle of the system, Equations (1) and (2).

Typical examples of this type of relaxation oscillations are the well-known oscillations of a control circuit consisting of a two-step controller with hysteresis and a first-order delay as relevant storage.

The literature on oscillations in chemical reactions is voluminous. Comprehensive reviews have recently been published by Sheintuch and Schmitz (1977) and Frank (1978). Most of the observed oscillations have relaxation characteristics and have been obtained under isothermal conditions.

This paper deals both with isothermal and thermal relaxation oscillations occurring in a loop reactor or a CSTR and in a catalytic fixed-bed reactor. The results are based upon theoretical considerations and simulation.

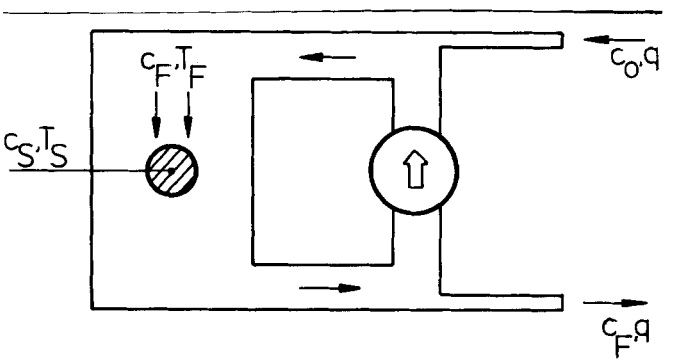

Fig. 3. Single catalyst pellet in a loop reactor.

THERMAL RELAXATION OSCILLATIONS IN A LOOP REACTOR

To explain the characteristics of relaxation oscillations in chemical reactors, we initially consider an exothermic reaction on a single catalyst pellet in a loop reactor (Figure 3). For a single reaction, the following balance equations for the catalyst pellet apply:

Mass balance in quasi steady state:

$$0 = \beta \frac{A_p}{V_p} (c_F - c_S) - r(c_S, T_S) \tag{3}$$

Energy balance:

$$(\rho c_p)_S \frac{dT_S}{dt} = \alpha \frac{A_p}{V_p} (T_F - T_S) + (-\Delta H_R) r(c_S, T_S) \tag{4}$$

If the reaction is strongly exothermic and of first order, the solution of the above equations yields a steady state rate dependency $r^*(c_F, T_F)$ as given in Figure 4 (see Horak and Jiracek, 1972).

It will be assumed that the gas temperature T_F in the reactor is kept constant. If the recirculation rate in the loop reactor is high enough, the gas concentration c_F is determined by the following mass balance equation:

$$V_R \frac{dc_F}{dt} = q(c_o - c_F) - \beta A_p (c_F - c_S) \tag{5}$$

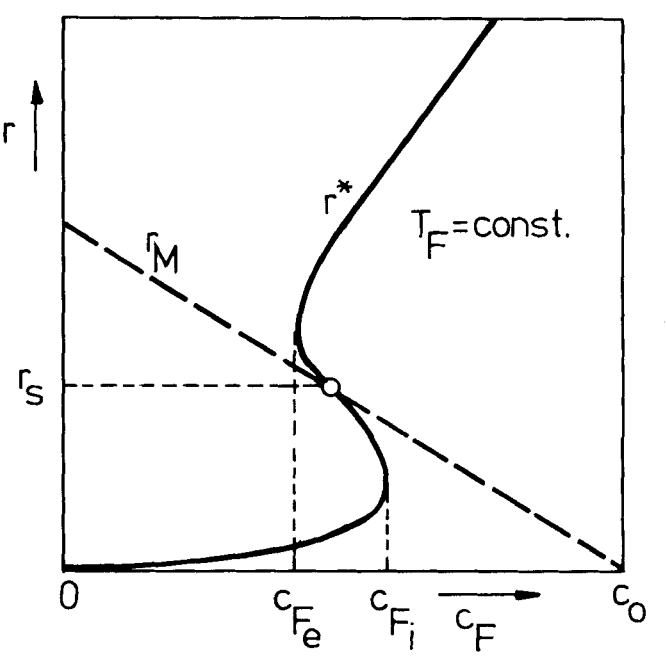

Fig. 4. Steady state rate dependency of the catalyst pellet r^* and transport line r_M of the loop reactor.

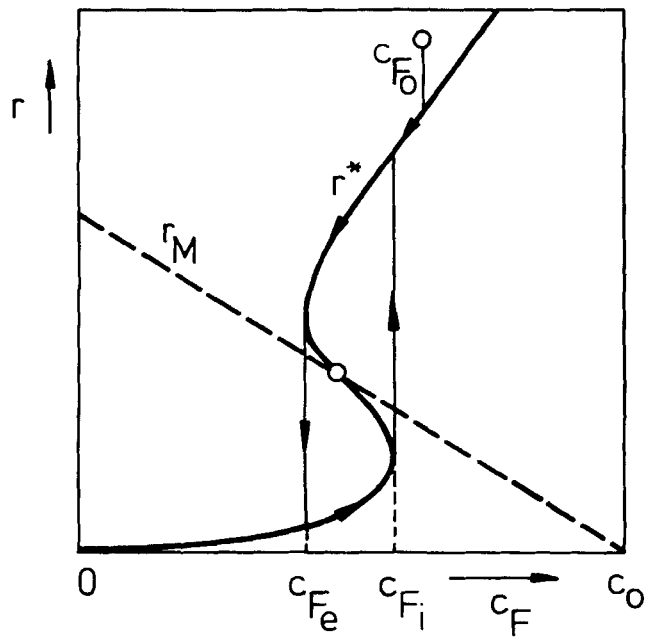

Fig. 5. Limit cycle of relaxation oscillations in the loop reactor.

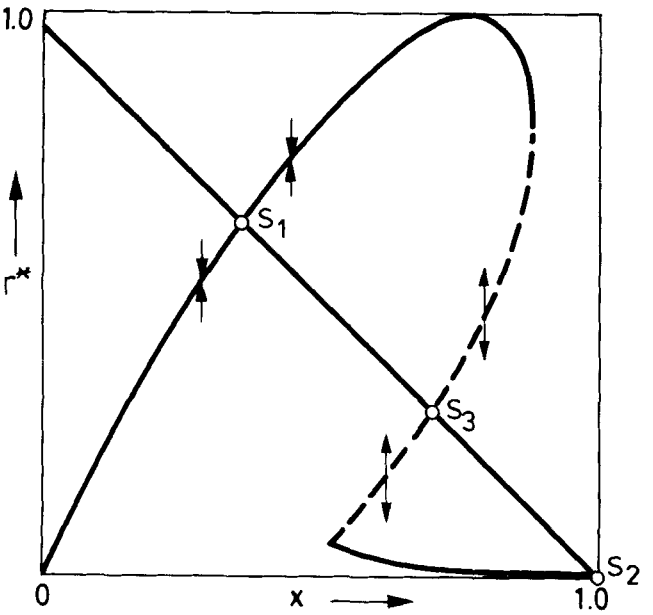

Fig. 6. Mass consumption curve and mass feed line (B in excess).

In the steady state, the relation

$$\frac{q}{V_p}(c_o - c_F) = r^*(c_F, T_F) \tag{6}$$

results (mass feed line r_M in Figure 2).

A decisive parameter for the dynamics of the system is the reactor volume V_R. If it is very large, the catalyst pellet will establish a quasi steady state corresponding to the current gas concentration c_F. If this state lies on the upper branch of r^* (Figure 5), the rate is higher than the steady state rate r_s; thus, c_F will slowly decrease and the quasi steady state moves to the left until with $c_F < c_{Fe}$, a steady state is only possible on the lower branch of r^* (the reaction dies out). Now the rate is lower than r_s; c_F slowly increases until c_F exceeds c_{Fi}. Then only the upper quasi steady state is possible, the reaction ignites and the depicted limit cycle develops (Figure 5). Horak and Jiracek (1972) have published experimental results with the hydrogen oxidation on a platinum catalyst pellet which closely reflect the above considerations.

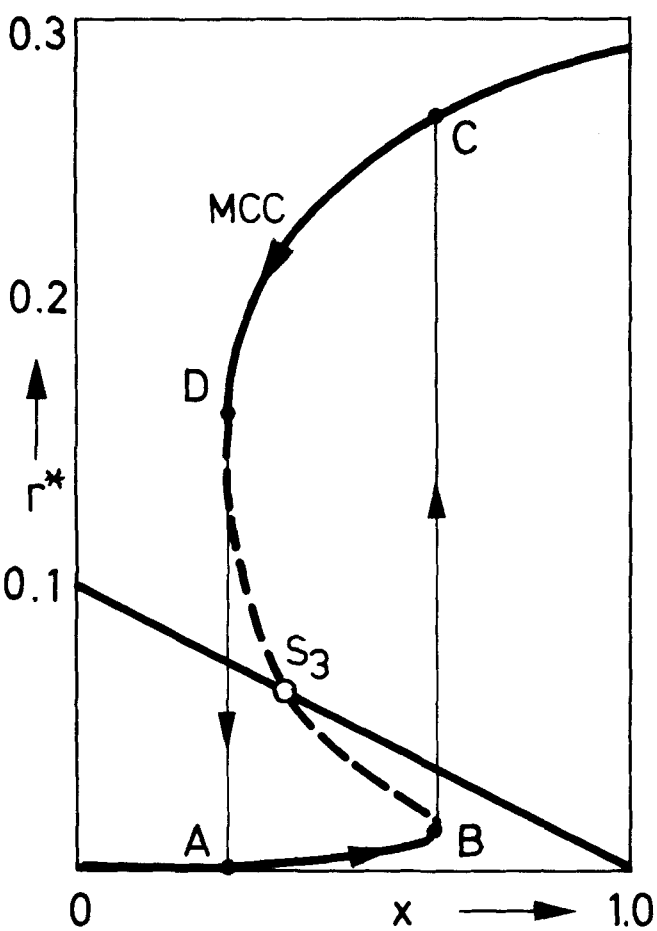

Fig. 7. Mass consumption curve and mass feed line (A in excess).

MASS RELAXATION OSCILLATIONS IN A CSTR

Let us next consider a CSTR or a loop reactor with the following catalytic surface reaction. [A similar reaction mechanism has been used by Eigenberger (1976) to model the carbon monoxide-oxidation on platinum.]

$$A + X \underset{k_{-1}}{\overset{k_1}{\rightleftarrows}} AX \tag{7}$$

$$B + 2X \underset{k_{-3}}{\overset{k_3}{\rightleftarrows}} BX_2 \tag{8}$$

$$AX + BX_2 \xrightarrow{k_2} C + 3X \tag{9}$$

where Equation (8) describes the assumption that the molecule B needs two active sites on the catalyst surface as for instance oxygen on platinum. To simplify the calculations, we consider the following case:

1. Step 8 is very fast in comparison to Equations (7) and (9).
2. $k_{-3} >> k_3 c_B$.

This leads to a more simple mechanism

$$A + X \underset{k_{-1}}{\overset{k_1}{\rightleftarrows}} AX \tag{10}$$

$$AX + B + 2X \xrightarrow{k_2} C + 3X \tag{11}$$

which shows in Equation (11) the self-accelerating influence of the active sites.

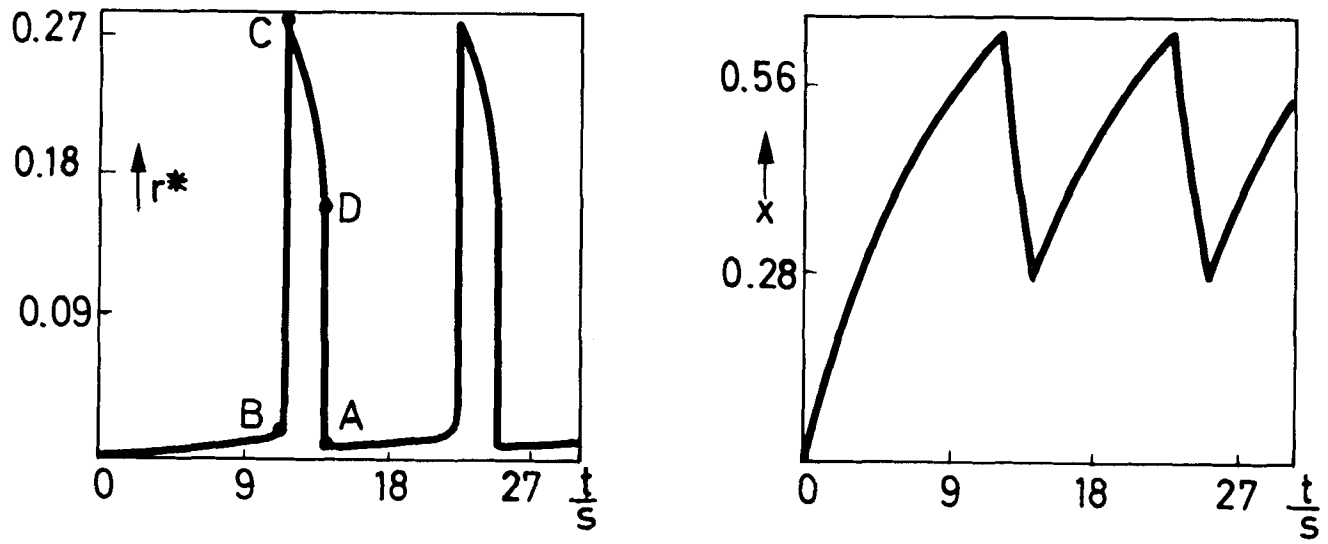

Fig. 8. Relaxation oscillation of a CSTR.

If it is presupposed that the time constants of the reaction are negligible compared with the residence time of the reactor, the concentration of AX is always in quasi steady state, and its mass balance yields

$$k_1 c_A (c_{Xo} - c_{AX}) - k_{-1} c_{AX} = k_2 c_B c_{AX} (c_{Xo} - c_{AX})^2 \tag{12}$$

where c_X has been replaced using $c_X = c_{Xo} - c_{AX}$.

Equation (12) is a nonlinear equation for c_{AX}. It is solved using a normalized form

$$\underbrace{k_1 c_{Xo} \frac{c_A}{c_{Ao}} (1 - \xi) - k_{-1} \frac{c_{Xo}}{c_{Ao}} \xi}_{r_A} = \underbrace{k_2 c_{Bo} \frac{c^3_{Xo}}{c_{Ao}} \frac{c_B}{c_{Bo}} \xi (1 - \xi)^2}_{r_B} \tag{13}$$

with $\xi = c_{AX}/c_{Xo}$. For each of the components A and B, a mass balance of the form

$$V_R \frac{dc}{dt} = q(c_o - c) - V_c r(c) \tag{14}$$

has to be considered. Two cases will be distinguished:

1. Component B in excess [c_B = const., $c = c_A$, $r = r_A$ in Equation (14)].
2. Component A in excess [c_A = const., $c = c_B$, $r = r_B$ in Equation (14)].

The mass consumption curves MCC, $r_A = r_A(c_A)$ for case 1 and $r_B = r_B(c_B)$ for case 2 can be obtained by elimination of ξ in Equation (13). Substituting

$$x = \frac{c_A}{c_{Ao}}, \quad r^*(x) = \frac{1}{c_{Ao}} r_A (c_{Ao} \cdot x) \quad \text{for case 1}$$

and

$$x = \frac{c_B}{c_{Bo}}, \quad r^*(x) = \frac{1}{c_{Bo}} r_B (c_{Bo} \cdot x) \quad \text{for case 2}$$

we get the MCC curves in Figures 6 and 7 which show the steady state solutions (S_i) of Equation (14) in a normalized form:

$$\frac{q}{V_c} (1 - x) = r^*(x) \tag{15}$$

Case 1 (B in excess) leads to one or, as shown in Figure 6, two stable steady states S_1 or S_2. This means a relaxation oscillation is basically impossible according to the general remarks stated previously.

In case 2 (A in excess), however, the feed line intersects only the unstable branch of the mass consumption curve, and relaxation oscillations occur in the reactor. The trajectory of this oscillation is composed of the section AB and CD of the stable branches of the MCC and the two vertical lines BC and DA.

Equations (13) and (14) have been simulated on a digital computer using the parameter values given in Figures 6 and 7. Typical simulation results of a limit cycle are shown in Figure 8. In the curves $r^*(t)$, the characteristic jumps in the reaction rate can be observed, whereas the normalized concentration $x(t)$ behaves like the temperature of a furnace controlled by a two-step controller with hysteresis.

THERMAL RELAXATION OSCILLATIONS IN A CATALYTIC FIXED-BED REACTOR

For the sake of simplicity, we confine ourselves initially to a reactor with a very short catalyst bed, so that the spatial dependency on the coordinate z may be neglected. The simplified equations of the catalyst bed are similar to the single pellet Equations (3) and (4):

$$(\rho c_p)_S \frac{dT_S}{dt} = \alpha \frac{3}{R_p} (T_F - T_S) + (-\Delta H_R) r(c_S, T_S) \tag{16}$$

$$0 = \beta \frac{3}{R_p} (c_F - c_S) - r(c_S, T_S) \tag{17}$$

The concentration is considered to be in a quasi steady state. For the rate of the reaction $A \rightarrow B$, the following rate dependence will be used:

$$r(c_S, T_S) = a_1 e^{-\frac{E}{RT_S}} \frac{c_S}{(1 + a_2 c_S)^4} \tag{18}$$

The concentration dependent section of Equation (18) shows considerable self-inhibition, as can be observed in the dehydrogenation or dehydration of some alcohols over oxide catalysts. In general, the coefficient a_2 is also dependent on the temperature. In order to show the basic behavior, a reaction rate with a_2 = const. is assumed. The aim is to construct a multivalued nonlinearity by eliminating c_S from Equation (17). The elimination can be carried

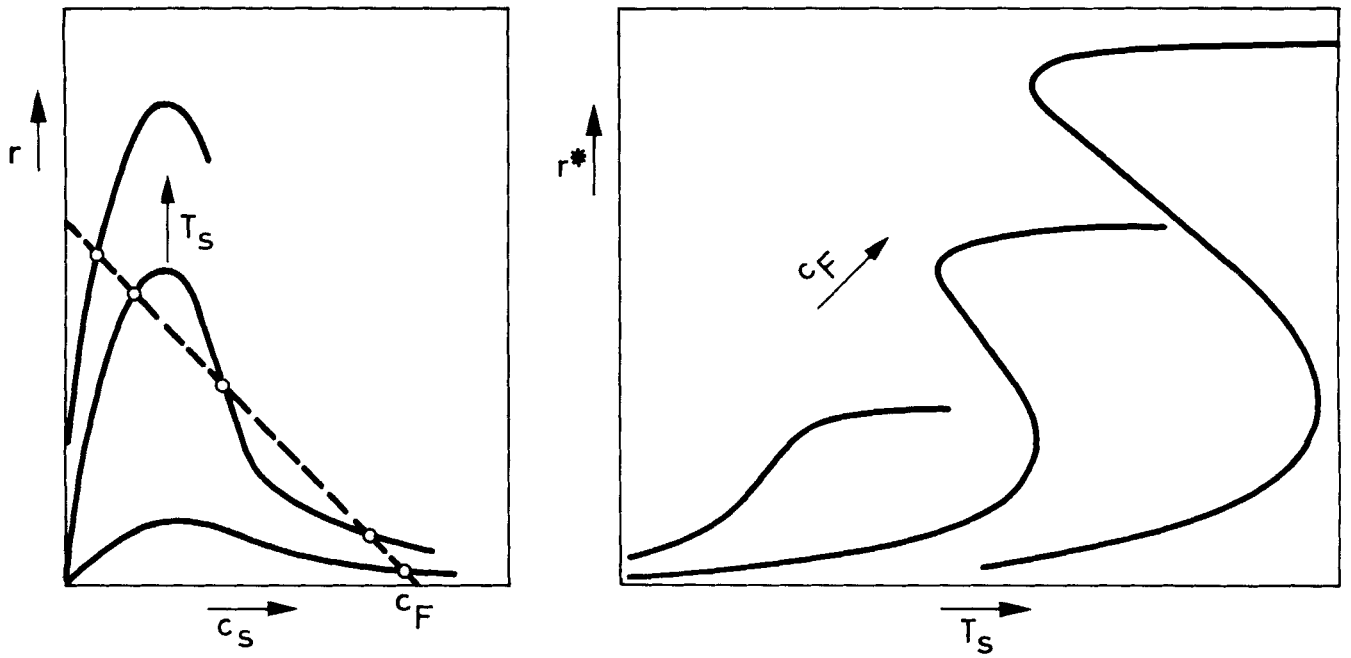

Fig. 9. Generation of the nonlinearity $r^*(c_F, T_S)$.

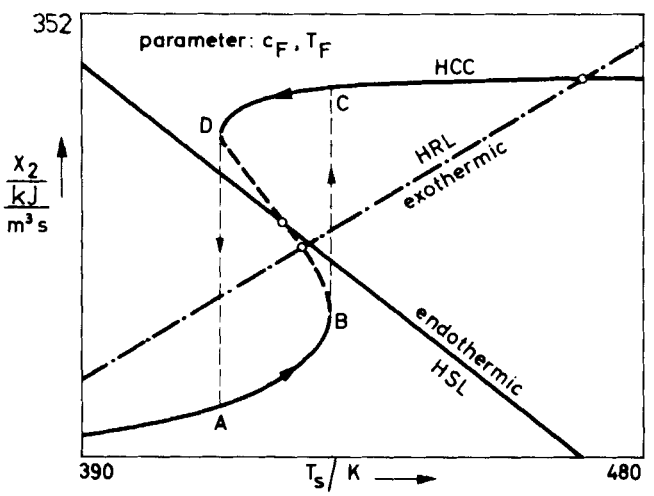

Fig. 10. Steady state solution and limit cycle of the differential reactor.

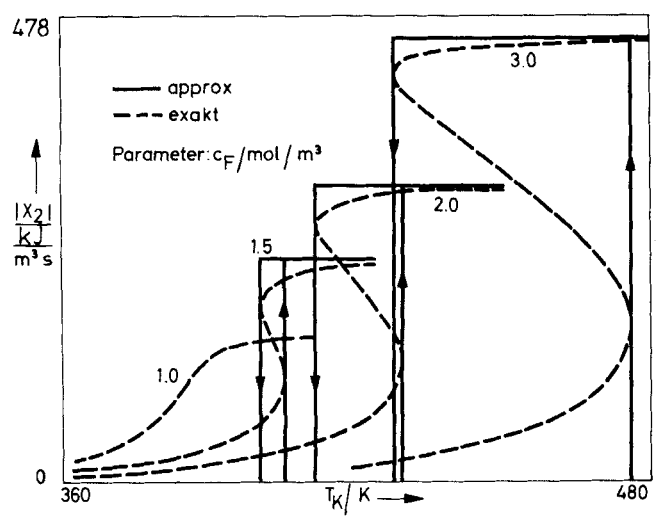

Fig. 11. Approximation of the nonlinearity $r^*(c_F, T_S)$.

out graphically by plotting the reaction rate $r(c_S, T_S)$ and the mass feed line $\beta\ 3/R_p(c_F - c_S)$ against c_S, as is shown in Figure 9.

If one increases the catalyst temperature, the maximum shifts upwards, and the projection of the intersection leads to the resulting reaction rate $r^*(c_F, T_S)$. r^* is essentially dependent on the fluid concentration c_F. A multivalued state cannot exist for small fluid concentrations. It develops when the concentration is increased. Then the hysteresis becomes more and more distinct.

The elimination of c_S leads to a first-order differential equation for the catalyst temperature T_S:

$$(\rho c_p)_S \frac{dT_S}{dt} = \underbrace{-\alpha \frac{3}{R_p}(T_S - T_F)}_{\text{HSL,HRL}} + \underbrace{x_2(c_F, T_S)}_{\text{HCC}} \quad (19)$$

Here

$$x_2(c_F, T_S) = (-\Delta H_R) r^*(c_F, T_S) \quad (20)$$

is the heat production or heat consumption curve (HCC) for an exothermic or endothermic reaction.

Figure 10 depicts the steady state solution of Equation (19), where the straight lines represent the heat removal line (HRL) in the case of an exothermic reaction and the heat supply line (HSL) in the case of an endothermic reaction. In the case of an exothermic reaction, the heat removal line HRL intersects either one or three times. If only one steady state exists, the reactor is asymptotically stable. If three intersections occur, the outer solutions are asymptotically stable, whereas the central one is unstable. Since there is at least one stable steady state, thermal relaxation oscillations cannot occur. If the reaction is endothermic, however, the situation changes drastically. x_2 is negative, and the heat supply line HSL in Figure 10 has negative slope. For a certain range of fluid temperatures T_F and fluid concentrations c_F, the heat removal line intersects only the dashed branch of the heat curve HCC. This means that a limit cycle will develop. The trajectory of this oscillation is given by the segments AB and CD of the stable branches of HCC and the straight vertical lines BD and CA. With at least one point of intersection located on a stable branch of HCC, the reactor is asymptotically stable.

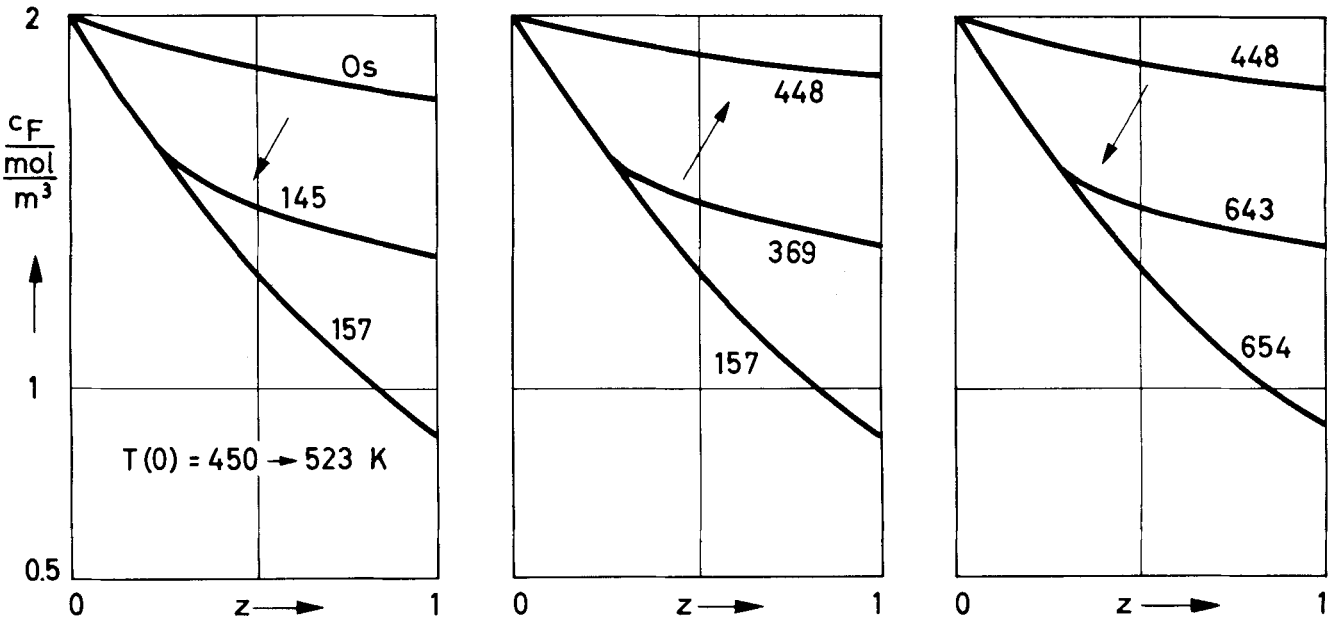

Fig. 12. Fluid concentration during the buildup of the limit cycle.

SIMULATION OF A FIXED-BED REACTOR

To simulate relaxation oscillations in a fixed-bed reactor of finite length, a simplified two-phase model which neglects any diffusion processes in the fixed bed is considered:

$$v\frac{\partial c_F}{\partial z} = -\frac{1-\epsilon}{\epsilon}\beta\frac{3}{R_p}(c_F - c_S) \tag{21}$$

$$v(\rho c_p)_F\frac{\partial T_F}{\partial z} = -\frac{1-\epsilon}{\epsilon}\frac{\alpha 3}{R_p}(T_F - T_S) \tag{22}$$

$$0 = \beta\frac{3}{R_p}(c_F - c_S) - r(c_S, T_S) \tag{23}$$

$$(\rho c_p)_S\frac{\partial T_S}{\partial t} = -\alpha\frac{3}{R_p}(T_S - T_F) + (-\Delta H_R)r(c_S, T_S) \tag{24}$$

with

$$c_F(0,t) = c_o,\ T_F(0,t) = T_o,\ T_S(z,0) = T_A \tag{25}$$

The following data were used:

Reaction:

Parameters	$a_1 = 3\cdot10^6$ 1/s
	$a_2 = 1\,500$ m³/kmole
Activation energy	$E = 41\,870$ kJ/kmole
Reaction enthalpy	$(-\Delta H_R) = -2.512\cdot10^5$ kJ/kmole

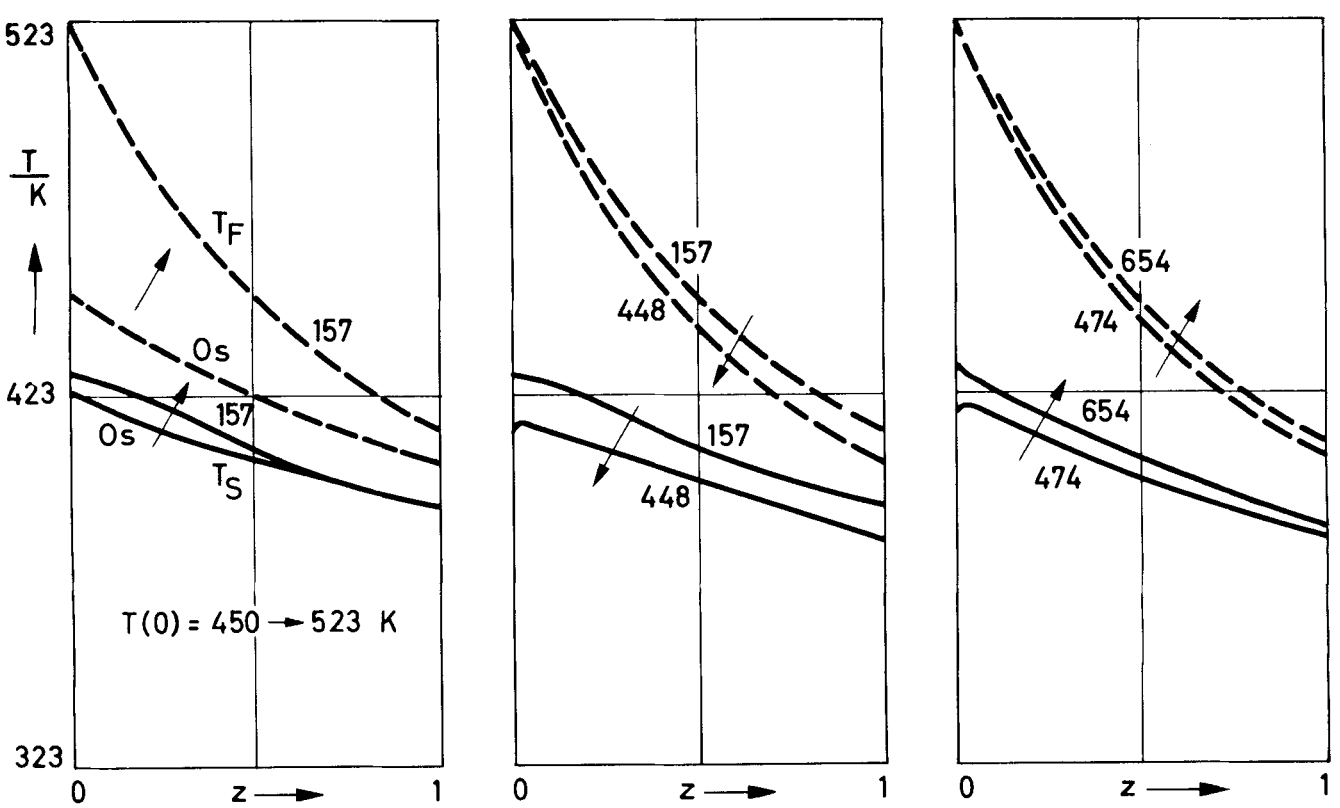

Fig. 13. Fluid- and catalyst temperature during the buildup of the limit cycle.

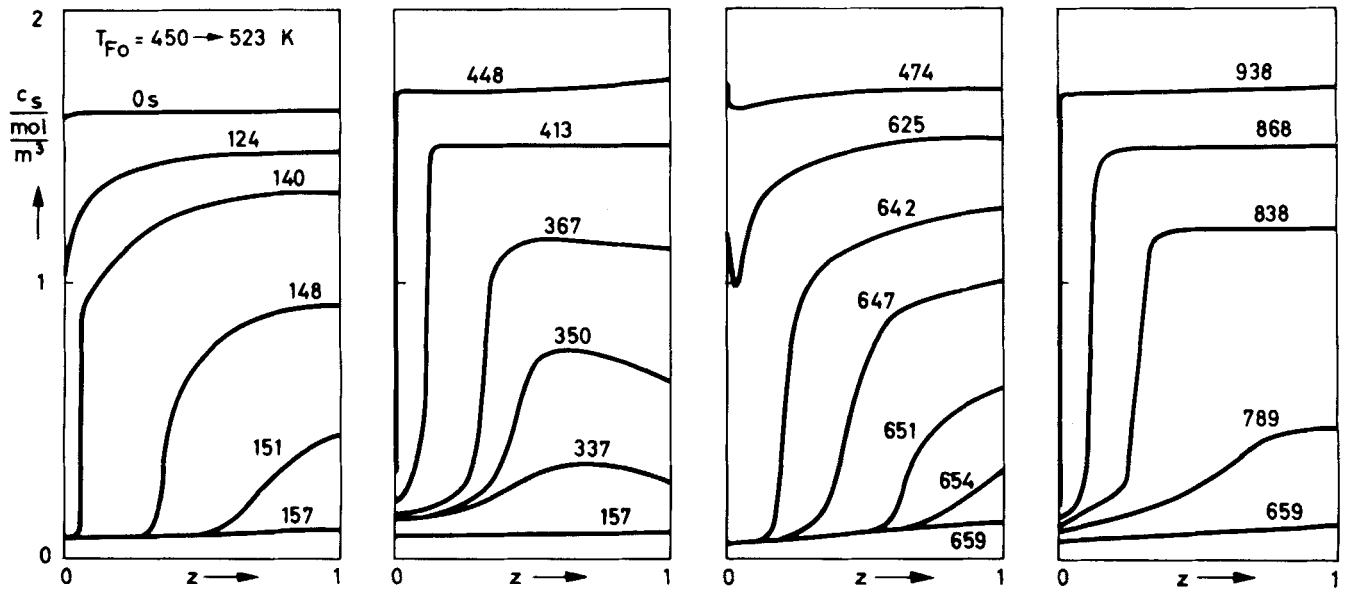

Fig. 14. Catalyst concentration during the buildup of the limit cycle.

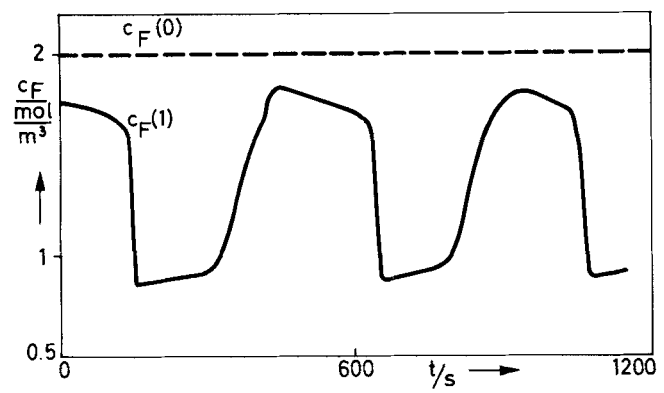

Fig. 15. Relaxation oscillations of the fluid concentration at the end of the fixed-bed reactor.

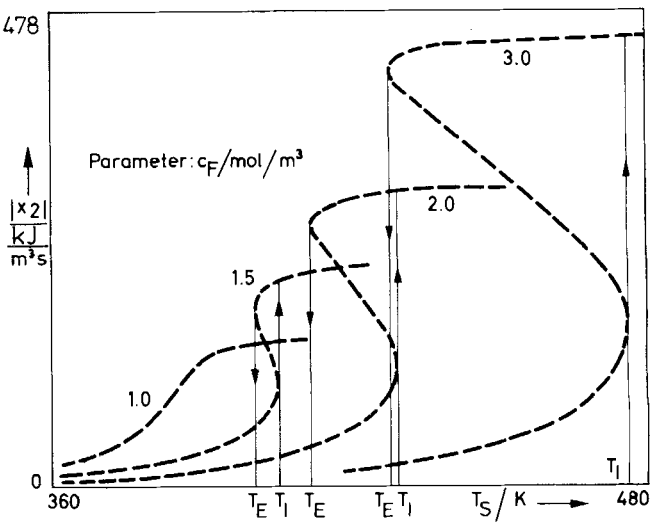

Fig. 16. Ignition and extinction temperature (T_I, T_E) in dependence of the fluid concentration c_F.

Reactor:

Length	l	= 1.5 m
Heat capacity of the fluid	$(\rho c_p)_F$	= 1.26 kJ/kg °K
Heat capacity of the solid	$(\rho c_p)_S$	= 1.256 kJ/kg °K
Heat transfer coefficient	α	= 2 kJ/m² °K*
Mass transfer coefficient	β	= 0.006 m/s*
Part of free space	ϵ	= 0.4
Radius of a pellet	R_p	= 0.003 m

Feed:

Flow velocity	v	= 1 m/s
Temperature	T_{Fo}	= 450 → 523°K
Concentration	c_{Fo}	= 2 mole/m³

In order to obtain a general picture of the behavior of the system, the Equations (21) to (25) were initially simulated with the aid of a very fast hybrid method of Ruppel and Zeitz (1975) in which Equations (23) and (24) are combined with Equation (19) through the elimination of c_S. The resulting multivalued heat consumption curves $r(c_F, T_S)$ can be approximated by means of a piecewise constant function as in Figure 11.

This procedure delivered the basic dynamic behavior of the variables c_F, T_F, T_S as was demonstrated by Gilles and co-workers (1976). The calculation of the concentration inside the catalyst phase c_S necessitated the simulation of the exact Equations (21) to (25) which was carried out using a digital method from Lübeck (1975).

Figures 12 to 14 show the spatial profiles of the temperature T_F, T_S and the concentrations c_F, c_S during the buildup of the oscillations spatial coordinate normalized. The process was started by increasing the feed temperature T_{Fo} from 450° to 523°K with a feed concentration c_{Fo} of 2 mole/m³.

As is shown in Figure 18, this disturbance causes a change from a stable solution to a point in the unstable region of the c_F, T_F plane characterized by a single steady state in the unstable branch of the nonlinearity $r^*(c_F, T_S)$. The resulting buildup of oscillations in the fluid concentration $c_F(1, t)$ at the end of the reactor are depicted in Figure 15.

In contrast to the smooth profiles of the fluid concentration and of both temperatures T_F and T_S, the catalyst concentration has a notable ignition/extinction behavior with very steep profiles. If the reactor is ignited by gradually raising the feed temperature, the reaction rate $r^*(c_F, T_S)$ jumps to a high value at the reactor front while remaining low in the rest of the reactor.

* In order to demonstrate pronounced relaxation oscillations clearly, very poor transfer coefficients were assumed. Unless indicated to the contrary, all results are based on these data.

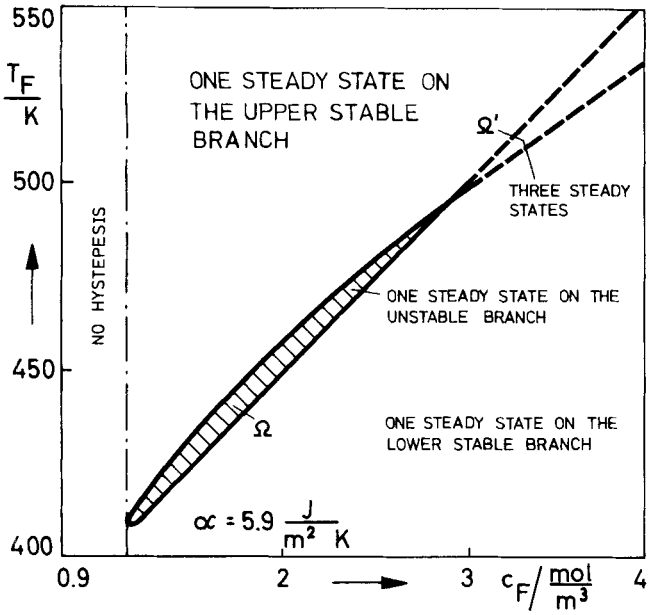

Fig. 17 Instability domain Ω of a fixed-bed reactor with an endothermic reaction.

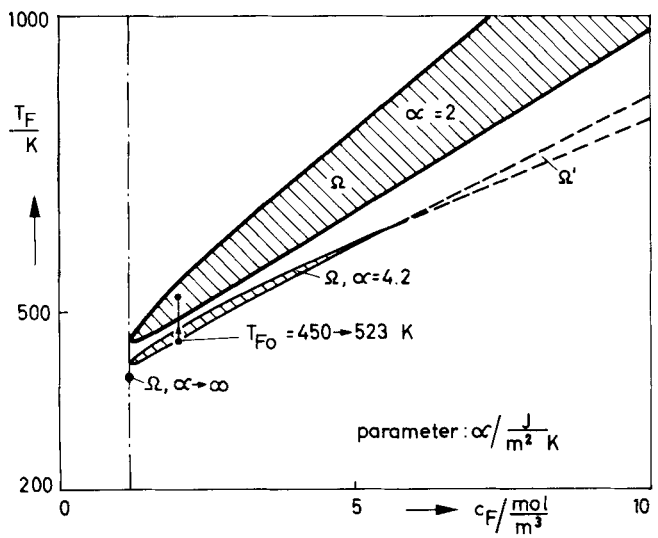

Fig. 18. Instability domain Ω as a function of the heat transfer coefficient α.

The fluid concentration in the bed decreases owing to the reaction, and hence (see Figure 16) the ignition temperature T_I of the reaction also decreases so that the reactor can ignite progressing in flow direction over the entire length. Thus, a sharply defined reaction front shifts from the front to the end of the reactor. In the ignited state, the catalyst temperature decreases owing to the heat consumption of the endothermic reaction, and hence the reaction rate is reduced. Consequently, the increasing fluid concentration leads to an increase in the extinction temperature until the reaction is extinguished at the position of the lowest temperature, namely, at the reactor end (Figure 16). A further increase in the fluid concentration shifts the extinction temperature to even higher values, so that a reaction front moves from the reactor end to the entrance.

The slope of the concentration profile in Figure 14 becomes steeper since the difference between the reaction rates in the ignited and nonignited parts grows larger with increasing fluid concentration. After the extinction of the reactor, the catalyst temperature increases as a result of the high temperature, until the reactor reignites.

GRAPHICAL CRITERION OF STABILITY

As was pointed out by Gilles (1976), a very simple stability criterion for an endothermic reaction can be formulated if the influence of heat conduction is neglected in the catalyst phase.

A difference approximation of the spatial coordinate leads to a splitting of the fixed-bed reactor into differential reactors with individual fluid temperatures and fluid concentrations. For each of these differential reactors, a steady state solution exists (Figure 10). Varying T_F results in a parallel shifting of the HSL, and a change in c_F influences the HCC as shown in Figure 9. Above a certain fluid concentration, the HCC is multivalued.

Moving the HSL from point B to D (Figure 10) leads to a temperature region $T_{F1,2}$ in which only one intersection in the unstable branch of the HCC occurs, and consequently oscillations are possible.

If the bounds $T_{F1,2}$ are plotted as functions of c_F, we obtain the hatched domain Ω of the c_F, T_F plane which is shown in Figure 17. This domain is characterized by the existence of relaxation oscillations. These results lead to a very simple stability criterion:

The reactor is asymptotically stable if the trajectory of the steady state profiles of the concentration c_F and the temperature T_F runs outside the domain Ω of the c_F, T_F plane. The reactor oscillates if the steady state trajectory enters or passes through the domain Ω.

The size of the region Ω is dependent on all parameters of the reaction and the transport processes. The simulation was based on a small value for the heat transfer coefficient α, $\alpha = 2$ J/m² °K. Increasing α causes the region Ω to contract until finally just a single point remains in the c_F, T_F plane (Figure 18). Hence for each α at least one point in the c_F, T_F plane exists which leads to oscillatory instability in the fixed bed reactor.

ACKNOWLEDGMENT

This work was supported by the Deutsche Forschungsgemeinschaft, for which the authors express their gratitude.

NOTATION

$a_{1,2}$ = parameters of the reaction rate r
A_p = surface of a pellet
c_y = molar concentration of the species y; $y = A, AX, B, X$
c_{yo} = value at the time $t = 0$
c_F = fluid concentration
c_{Fo} = value in feed to reactor
c_S = concentration of the catalyst phase
E = activation energy
k_i = rate constant
q = volumetric flow rate
r, r^* = reaction rate
R = ideal gas constant
R_p = radius of a pellet
t = time coordinate
T_A = temperature inside the reactor at the time $t = 0$
T_F = fluid temperature
T_{Fo} = value in feed to reactor
T_S = temperature of the catalyst
v = flow velocity
V_c = catalyst volume
V_p = volume of a pellet
V_R = reactor volume
x = active site
z = space coordinate

Greek Letters

α = heat transfer coefficient
β = mass transfer coefficient
$(-\Delta H_R)$ = reaction enthalpy
ϵ = part of free space in the fixed bed
$(\rho c_p)_F$ = heat capacity of the fluid
$(\rho c_p)_S$ = heat capacity of the catalyst
$\xi = c_{AX}/c_{Xo}$ = dimensionless concentration of the chemisorbed species A

LITERATURE CITED

Eigenberger, G., "Mechanismen und Auswirkungen kinetischer Instabilitäten bei heterogen-katalytischen Reaktionen," Habilitationsschrift, Universität Stuttgart, West Germany (1976).

Fieguth, P., and E. Wicke, "Der Übergang vom Zünd-/Lösch-Verhalten zu stabilen Reaktionszuständen bei einem adiabatischen Rohrreaktor," *Chem. Ing. Techn.*, 43, 604 (1971).

Frank, U. F., "Chemische Oszillationen," *Angewandte Chemie*, 1, 1 (1978).

Gilles, E. D., "Reactor Models, Fourth International Symposium on Chemical Engineering," Heidelberg (1976).

———, G. Eigenberger, and W. Ruppel, "Relaxation Oscillations in Chemical Reactors," paper presented at AIChE Meeting, Chicago, Ill. (1976).

Horák, J., and F. Jirácek, "A study of the dynamic behaviour of catalytic flow reactors," II. Int. Symp. Chem. Reaction Engng. Amsterdam, B8-1, Elsevier (1972).

Lübeck, B., "Kontinuierliche Modelle katalytischer Festbettreaktoren und ihre digitale Simulation mit Integralgleichungen," Dissertation, Universität Stuttgart, West Germany (1975).

Ruppel, W., and M. Zeitz, "Implicit Simulation Method for Distributed Parameter Systems on a Hybrid Computer," *Proc. Intern. Assoc. Analog Computation*, 3, 1 (1975).

Sheintuch, M., and R. A. Schmitz, "Oscillations in Catalytic Reactions," *Catal. Rev.-Sci. Eng.*, 15, 107 (1977).

Manuscript received September 12, 1977; revision received May 30, and accepted June 21, 1978.

Transient Gas-Liquid Flow in Horizontal Pipes: Modeling the Flow Pattern Transitions

The theory for predicting flow pattern transition under transient flow conditions is developed and compared with experiment. This work represents an extension of the methods presented by Taitel and Dukler (1976) for steady state flows. Under transient conditions, flow pattern transitions can take place at flow rates substantially different than would occur under steady flow conditions. In addition, flow patterns can appear which would not be expected for a slow change in flow rates along that same path. Methods are presented for predicting the flow rates at which flow pattern transitions will take place during flow transients. The method also reveals when spurious flow patterns will appear.

YEHUDAH TAITEL
NAUGAB LEE
and
A. E. DUKLER

University of Houston
Houston, Texas 77004

SCOPE

During a concurrent gas-liquid flow in horizontal pipes, a variety of flow patterns can exist. Each pattern results from the particular manner by which the liquid and gas distribute in the pipe. Most observers classify the variety of observed distributions into six patterns as shown in Figure 1 (Govier and Aziz, 1972; Hewitt and Hall-Taylor, 1970). Rates of transport of energy and mass between the two phases as well as between the individual phases and the wall vary greatly with flow pattern. Given the steady state flow rates of the two phases, the fluid properties and the tube size, a central task to those attempting to model the two phase transport process or to design two phase flow equipment is to predict the particular flow pattern which will exist and the flow rate pairs at which transition between flow patterns will be observed. Figure 2 is an example of a flow pattern map for steady air-water at low pressures in 2.0 to 3.0 cm diameter pipes. The locus of the flow rate pairs at which transition takes place are shown.

In many cases of industrial interest, the flow rates vary with time. Examples include start-up or shutdown of process equipment, changes in flow rates in response to changes in planned operating conditions, and emergencies such as rapid depressurization of equipment due to accident conditions. A case of particular importance is that of a nuclear reactor under conditions of a loss of coolant accident. It is often essential to be able to predict the flow regimes during the transient. If a very slow change is made from one flow rate pair to a second and the path crosses several transition curves (Figure 2), experience has shown that the flow pattern transitions take place at the same flow rates as would be expected for equilibrium or steady flow. However, the same result is not observed for rapid transients.

It is the objective of this work to model the process of flow pattern transition under transient flow conditions, to provide methods for predicting such transitions, and to test the result against experiment.